CORNISH, L.A., GRANT, M., WILLIAMS, B., WILSENACH, I., and MCALLISTER, H. An evaluation of steels selected for use within electric arc furnaces. *The 4th International Platinum Conference, Platinum in transition 'Boom or Bust',* The Southern African Institute of Mining and Metallurgy, 2010.

An evaluation of steels selected for use within electric arc furnaces

L.A. CORNISH*, M. GRANT†, B. WILLIAMS†, I. WILSENACH†, and H. MCALLISTER†
**DST/NRF Centre of Excellence in Strong Materials and School of Chemical and Metallurgical Engineering*
†Enviroplus Design

In October 2008, a new 3 MW platinum furnace started running at Mintek's premises in Randburg. Enviroplus designed, built and commissioned the off-gas conditioning system for the furnace. At the time it was noted that the conditioning system, consisting of a water-cooled off-gas spigot on the furnace, followed by a water-cooled combustion section, ran virtually trouble free, but after 8 months of operation the off-gas spigot had suffered considerable corrosive pitting, indicating that a change of material, from 316L to some other steel, was necessary. Test coupons of various steels were welded into the inside jacket of the spigot and allowed to function during normal furnace operation for several months. The examination of these plates is presented, together with ongoing work to find the correct steel to ensure that the spigot will not suffer a material failure between major, once-a-year, overhauls of the furnace.

Introduction

In October 2008, a new 3 MW DC arc furnace started running at Mintek's premises in Randburg. Enviroplus designed, built and commissioned the off-gas conditioning system for the furnace. As anthracite is used as a reductant in the furnace, the off-gas is a highly flammable mixture of hydrogen and carbon monoxide which must be oxidized and cooled. Thermodynamic calculations also confirmed that the gases have high CO and H_2 content[1]. The values were calculated as: 57.6% CO; 32.9% H_2; 6.2% N_2; 3.3% SO_2 (volume %), and a flow rate of 0.27 t/h. An off-gas spigot and flame hood is followed by a water-cooled ducting section where combustion and gas cooling takes place. The design is such that the flow is laminar to ensure that the combustion occurs in the centre of the flow, and not at the wall edges, and all evidence has shown that this has been achieved. The maximum temperature expected in the furnace itself was 1 600°C, and so additional cooling air is introduced at the inlet of the water-cooled ducting section. Gas is then led through a trombone cooler to an existing baghouse for removal of furnace generated dust. From the baghouse, gas is routed through to a Venturi scrubber for conditioning before entering an SO_2 absorber, where it is reacted countercurrent with a caustic scrubbing solution. The cleaned gas is then exhausted from the system, via the ID fan to the stack. To date, no significant SO_2 emissions have occurred with the integrated gas conditioning/scrubber system on line and operating in normal mode. The slag is tapped at 1 650ºC, and the alloy is tapped at 1450ºC[1].

At the furnace roof off-gas outlet is a water-jacketed spigot that directs gas flow into the combustion section. The spigot seals the top of the furnace, allowing the furnace to operate under completely reducing conditions. Minimal blow-back or oxidizing conditions have been experienced in the furnace since commissioning, which was the case before the spigot was fitted. Additionally, there has been no need for regular cleaning to occur since the spigot was fitted. A 'freeze layer' of dust and condensed fume forms on the inner surface of the spigot. This assists with protection against the intense radiation from the molten bath. Should the layer build up, a swing-out combustion duct section, located above the spigot, creates access for off-line cleaning. A deliberate decision was made not to use a refractory material inside the spigot as this promotes a build-up of sintered material which is difficult to clean. Regular cleaning increases mechanical wear which before the design was changed, was necessary at least once per shift.

On 27 March 2009, there was a matte tap hole run-out experienced by the furnace, and a significant amount of radiant heat was released outside the furnace, damaging the operation area. During the run-out, the water cooling system was allowed to remain in service, and this probably saved the off-gas equipment. Enviroplus suggested that a visual inspection of the water-cooled duct in close proximity to the furnace should be done, with the possibility for non destructive testing (NDT) of certain components, based on the outcome of the visual inspection.

This inspection occurred on 3 April 2009. On the section of the combustion zone just above the swing-out section, a 1–2 mm internal build-up had occurred. Here, the underlying 316L stainless steel plate is 6 mm thick. When chipped away this revealed bare metal underneath. There was also no sign of sulphur build-up, indicating that laminar flame conditions did not allow contact of molten fume with the duct walls. However, on the outer ridge of the spigot, after removing the concentrate crust, sulphates had been deposited. There was a 'freeze layer' of dust and condensed fume formed on the inner surface. It was observed that the spigot had suffered no mechanical damage from the run out. However, several recommendations were made at the time, and these included

periodic maintenance to remove sulphur build-up; replacing the water supply and return hoses; not to undertake *in situ* NDT (because of difficulty in accessing the part, and the possibility of damaging it). It was also recommended that a spare spigot be made, so that one could be studied and one could be in service.

Water leaks due to severe coarse pitting was observed on the 316L stainless steel inner spigot surfaces after 7 months of service (excluding 6 weeks shutdown for the taphole run-out), and this was assumed to be due to the sulphur. It was decided to refit the spigot with new plates of 316L at the bottom. Simultaneously, a comparative experiment would be run using four different types of steel. Two coupons each of the selected steels were supplied to be welded to the 316L repair and the 316L substrate on the opposite side. These were 304, 3CR12, 2205 and plain carbon steel. This would allow a comparison of five different types of steel, including the 316L. So that the coupon test pieces could be easily recognized, they were cut into distinct shapes. These test pieces were installed on opposite faces so that the same steel could be compared in slightly different environments: close to the arc and further away from it. No details were given of the welding.

The installation was completed in July 2009, and the operation resumed for about a month before it was shut down due to raw material delivery problems. In October the operation resumed smelting material with significantly higher sulphur content, and ran for 4 months of apparently trouble-free operation before the spigot developed another water leak. Unfortunately, the spigot was not considered repairable and it was decided to plug the cooling circuits and refractory line the interior. The furnace operation was halted at the end of March 2010 because of lack of feedstock for processing. Mintek then kindly allowed the spigot to be available for inspection, and it was brought to the University of the Witwatersrand. It was assumed that the spigot was probably coated on the fire side with furnace dust and slag spatter.

During operation, it was stated that burning of the off-gas was not always consistent. Although this should have occurred above the spigot, occasionally the back-burn flame regressed into the spigot. This would have increased the temperatures. During operation, there were occasional shutdowns for cleaning of the entire system.

Investigation

Initial inspection

The spigot as it appeared on arrival at the University of the Witwatersrand is shown in Figure 1, and the water cooling had been disabled and plugged. Thus, the spigot would have reached much higher temperatures than had been designed for. It was also observed that the base was deformed (Figure 2), although this was later established to have been as a result of subsequent handling and not temperature.

It was also seen that part of the top had been removed, as shown in Figure 3, and looking down inside the spigot, the coating inside was both thicker and coarser than had been observed in the first inspection in April 2009.

The coarse deposit was removed using a wooden dowel, and eventually, one coupon test piece was found and two stubs on the side away from the arc. This was the 2205 coupon, and is shown in Figure 4. It was also observed that the plate to which the coupons had been welded was in reasonable condition. The coupons and part of the substrate that they had been attached to was removed for metallographic examination. Higher up in the spigot was refractory casting, which had also been added at the previous failure. No evidence of the coupons was found on

Figure 1. Blocked water-cooling mechanism

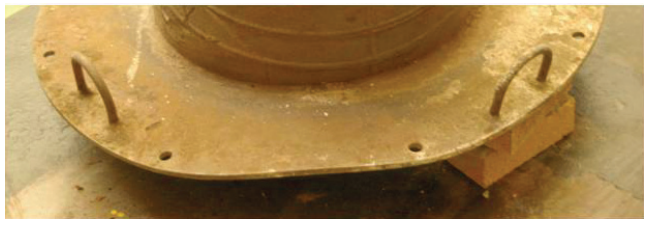

Figure 2. Deformed base of the spigot

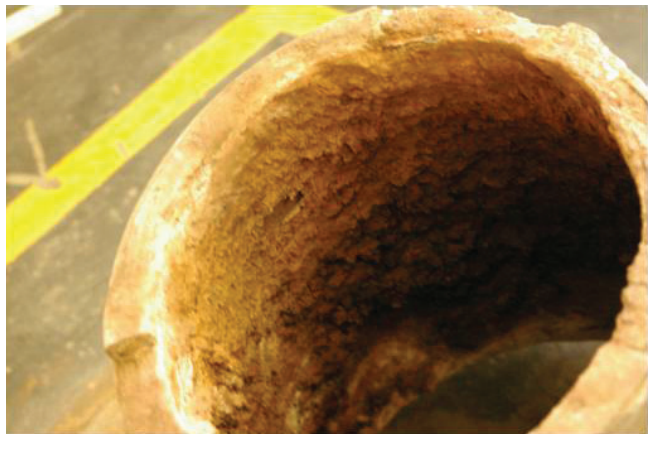

Figure 3. Top of the spigot showing the cut region and thick deposit inside the spigot

the side of the arc, nor could it be discerned whether the welds had failed.

Metallographic examination

The remaining coupons and a specimen from the 316L repair were removed and prepared metallographically so that the cross-sections through the samples to the surface could be studied. These were etched in oxalic acid after observing the unetched microstructures. Apart from the 316L specimen, no other unetched specimen showed discernable features. After etching, the two unidentified coupons were identified from their microstructures.

Although the initial coupon thicknesses were not given, it was assumed that they were of similar thickness. Comparing the thicknesses: the carbon steel was lost completely, 3CR12 was then thinnest, then 304, and lastly 2205. Thus the corrosion resistance was (starting with the highest):

2205 > 304 > 3CR12 > carbon steel.

Taking the 316L repair into account, it appeared to be fairly less affected on a macro-investigation, but was peeling off (Figure 8), and so the sequence would be:

2205 > 316L > 304 > 3CR12 > carbon steel.

Grain boundary corrosion was clearly seen in the unetched 316L specimen, and the precipitation of carbides could be seen at the grain boundaries beneath the surface (Figure 5). This is classic intergranular corrosion, which can occur after sensitization. In the spigot, there could be residual stresses resulting from thermal cycles, but the high running temperatures would offer *in situ* annealing. Although the furnace did run smoothly, there were maintenance periods where the furnace was cleaned. There were also pits and corrosion products shown as broken layers on the outside. Also present were internal nodules of graphite, identified by their appearance in the unetched micrograph.

The etched sample showed that there was also spalling, with corrosion products spreading underneath the substrate. The grains near the surface appeared much larger than those further in (Figure 6). However, this was more because the uneven precipitation of the carbides on some of the grain boundaries only.

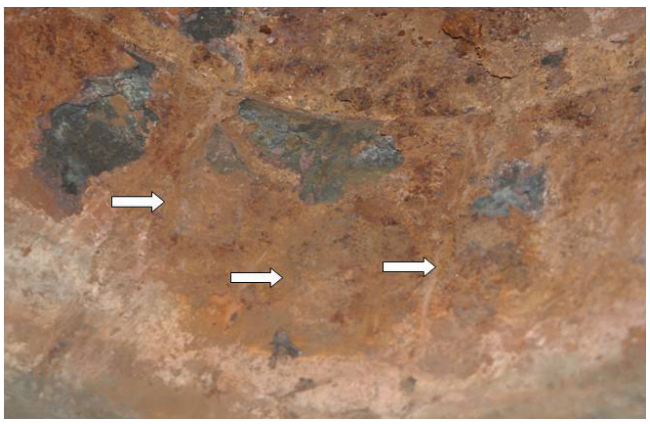

Figure 4. View inside the spigot showing the only coupon that was recognizable (left hand arrow), with the stubs of two other pieces (central and right arrows), all welded on new material near the base

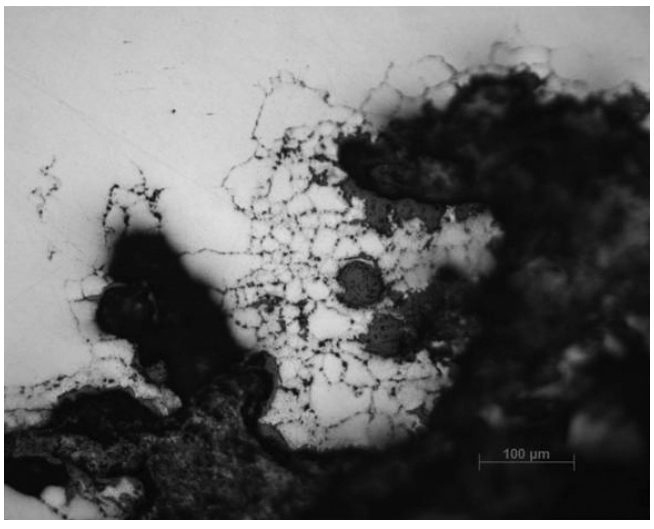

Figure 5. Optical micrograph of unetched 316L showing grain boundary corrosion and the precipitation of carbides at the grain boundaries

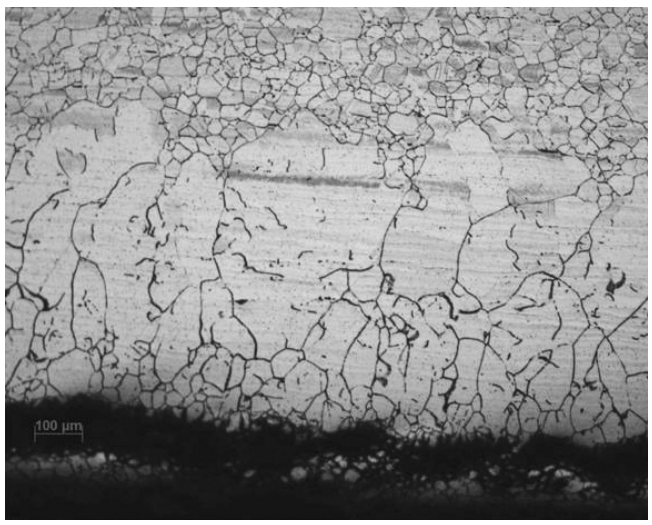

Figure 6. Optical micrograph of etched 316L sample showing carbide precipitation and apparent grain growth at the surface

Figure 7. Optical micrograph of etched 304 sample showing grain boundary corrosion and some precipitated needles

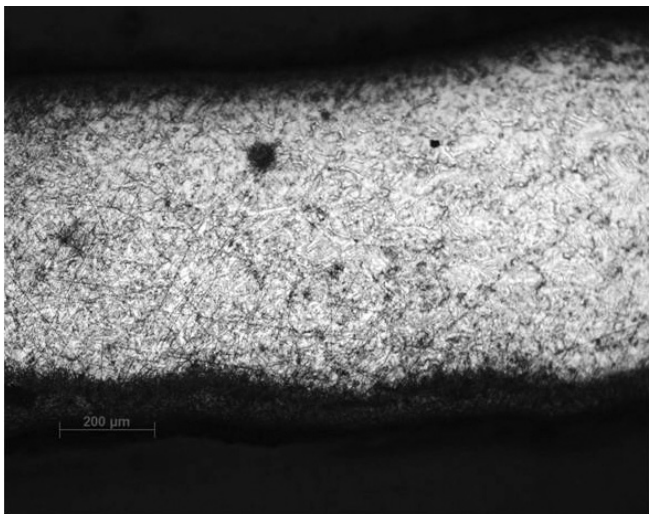

Figure 8. Optical micrograph of 3CR12 showing the dual phase nature (comprising ferrite and martensite) and layered surface (at the bottom)

Figure 9. Optical micrograph of 2205 sample, showing fine grain size, with carbide precipitation (dark) and a scale and grain boundary corrosion at the top

The 304 sample also showed sensitization and grain boundary corrosion; higher sensitization than in 316L would be expected from the nominal C contents. The annealed nature could also be seen with the high number of annealing twins, which is unsurprising considering the high temperatures to which the spigot was exposed. There were also some dark needle precipitates (Figure 7).

The 3CR12 sample did not prepare well, although the dual nature could be seen, together with a layered surface that was exposed (at the bottom of Figure 8.)

Of the experimental coupons, 2205 showed the best results. It was the only one that could be identified from its original shape, and it was also the thickest coupon. The surface also looked intact, although with a dark scale. The microstructure shows that there was a scale and the surface had deteriorated. The fine grain size, still in the original as-rolled, elongated morphology, as well as carbide precipitation away from the surface could be seen (Figure 9). There was also a stained region that was a shallow pit. There was some intergranular corrosion, but the depth was less than the other steels.

For a rough comparison, the coupon thicknesses and scale thicknesses are given in Table I. For thicknesses, the 316L repair plate cannot be compared with the others, since it had an unknown starting (and obviously thicker) thickness. The starting thicknesses of the coupons were stated to be 4 mm, but it is likely that they were actually 6 mm thick, since the 2205 sample was ~5 mm after exposure.

Discussion

It was obvious from the initial examination that the spigot was in a different condition from expected. With the water-cooling effectively plugged, the whole spigot would have reached much higher temperatures than originally anticipated in the design. These higher temperatures also meant that the deposit was able to build up into thicker layers than were anticipated. It must be noted that all the steels were being used at much higher temperatures than is usual, but that there had been no temperatures recorded in the spigot during operation.

Regarding the coupons, on the side nearest the arc, none was found, and this meant that the conditions were too severe for these to survive, or that the welds had failed. (No information was available on the welding.) This was initially surprising because it was expected that this region would actually be more sheltered. The 2205 coupon was the only one on the opposite side to survive intact, although two stubs were also found which were too corroded to be identified by their shape, and showed that the welds had not failed. One coupon was missing totally, and could have fallen off from the left side of the 2205 coupon (Figure 4).

An on-site report had considered various possible routes to failure[2]. These included periodic insufficient water for cooling which would cause thermal stress failures, and water washing of internals (due to excessive velocities of cooling water and/or corrosion). Although the first is definitely a possibility, the second could be discounted, because the water cooling was disabled. Sulphidic corrosion on the exposed surfaces of the spigot was also a possibility, although the freeze lining of slag/concentrate that formed on the inner surface exposed would have offered some protection. Although migration of sulphur compounds through the freeze lining is known[2], the (6 mm)

Table I
Summary of sample thicknesses and scale thicknesses

Sample	Sample thickness (mm)	Approximate grain size (µm)	Approximate scale thickness (µm)	Approximate depth to which intergranular corrosion penetrated (µm)
316L	7	~40	Patchy: ~200	Patchy: ~300
304	2	~150	Patchy: ~200	Patchy: ~300
3CR12	~1	~100	~80	~40
2205	5	~800	~30	~30

thickness of the 316L stainless steel plate, and the expected rate of corrosion at <0.1 μm per year should not have allowed this mechanism to affect the steel. The possibility of carbon reduction was mooted[2], and is postulated to originate from the direct reduction of iron (DRI) in a reducing environment. Hydrogen and carbon monoxide are reductants in the DRI process, and both were present in the operation of the furnace. These processes usually occur over temperature ranges of 650–950°C, and the end product is iron carbide, which is powdery and easily removed. However, the rate of reaction on stainless steels is less known. Hydrogen embrittlement is another process, and the free radicals of hydrogen can be produced at elevated temperature during their removal from the coal/char substrate, although the likely temperatures here would have been higher than usual for hydrogen embrittlement. The free radicals have high mobility at the atomic level, and easily penetrating steel[2].

The original steel, 316L stainless, was selected because it is a well-known grade to source and easy to fabricate. Its properties include a penetration rate below 0.0088 mm per month in carbon monoxide gas up to 870°C although no data were given for H_2S and H [3]. In the selection and repair, low carbon alloys were preferred because of their better performance.

The three other steels included an austenitic stainless steel (304), a chromium-containing corrosion resisting steel (3CR12), a duplex stainless steel (2205), and a plain carbon steel. The duplex stainless steel, with the correct 50:50 austenite: ferrite microstructure should have superior properties to both 304 and 316L in terms of stress corrosion cracking resistance as well as resistance to both pitting and crevice corrosion. Pitting usually occurs in the presence of chlorides. Since there are various embrittling reactions that occur at high temperatures, due to the precipitation of deleterious phases, the application temperatures, under force, are usually below 300°C[4]. The 2205 stainless steel is often recommended for environments with chlorides and H_2S.

Using a simplified pitting resistance equivalent (PRE) of PRE = Cr + 3.3 Mo + 16 N (wt%), and the steel compositions (Table II) the PREs of the three stainless steels considered here are (rounded up): 13 for 3CR12; 22 for 304; 30 for 316L and 38 for 2205. Thus, 2205 should have superior pitting resistance compared to the other stainless steels considered here, and the order agreed with the findings. In comparison, the carbon steel would have had negligible pitting resistance. Usually, Cr, Ni, Mo, Ti, Nb and N increase the pitting resistance, whereas Si, S and C have the opposite effect.

Considering the protection against sulphidation, the higher the chromium content, the better the protection will be. Type 316L has been shown to be effective against SO_2, but an H_2S is more demanding and needs a Cr content of at least 17 wt% Cr, which means that 304 stainless steel is often considered adequate.

It is evident from the external appearance that the spigot was in a much worse condition in May 2010 than it had been in April 2009. On the first occasion, there was coarse pitting on the inner surface of the 316L, and on the later occasion, there was a complete cover of deposit, up to ~15 mm thick, but underneath the 316L had survived well. This indicates strongly that the conditions were different, and apparently there were different mechanisms occurring. In the first case, the water cooling failed after 6 months of operation (October 2008–March 2009) whereas in the second case the repair failed after 4 months of operation (October 2009–January 2010) and operation was continued for an additional 2 months with water cooling. The temperatures were presumably higher during the later part of the second operation, because of the blocked water-cooling system.

The spigot was exposed to high temperatures, a reducing environment and a mixture of CO, H_2, N_2, SO_2, with smaller amounts of O_2 and H_2O gasses. These constituents can give rise to different corrosion mechanisms.

In order to understand the corrosion occurring inside the spigot, a review of the corrosion that has been reported in the steels under similar, or as near as possible, conditions is necessary. Grain boundary corrosion (intergranular corrosion), which is often caused by sensitization is a well-known problem for stainless steels. Besides degradation in corrosion resistance, sensitization could also promote stress corrosion cracking[5,6], although here the branching of the crack is less in stress corrosion cracking. The most accepted theory on the root cause of sensitization in stainless steels is the Cr-depletion theory[7,8], which dates back to the 1930s[7]. However, while $M_{23}C_6$ causes intergranular attack in most cases, other phenomena may lead to Cr depletion in grain boundaries, and Padilha *et al.*[9,10] found that $M_{23}C_6$ disappears in 316LN after very long-term ageing at 600°C. The situation is actually more complex[11,12], because other phases are involved.

The grain size will also have an effect, because of the ease of diffusion along the grain boundaries. Thus, as the grain size decreases, the time required for desensitization becomes shorter[13,14]. Eventually, the time lag between sensitization and desensitization will be negligible at sufficiently small grain sizes, because: many grain boundaries enables very efficient Cr diffusion, and also the distances for Cr to diffuse from grain interiors to the grain boundary regions are very small. Both factors facilitate the replenishment of Cr in the grain boundary Cr depleted regions, and so desensitization occurs almost simultaneously as sensitization.

Stainless steels are sensitive to metal dusting. Metal dusting is a high temperature corrosion phenomenon which causes the materials to disintegrate into a dust of fine metal particles, graphite, carbides and oxides[15,16,17]. Metal dusting is reported to occur between about 400 and 900°C, and metals are saturated with carbon and then disintegrate

Table II
Specifications of the steels used for the coupons

	Chemical composition (wt%) (Balance = Fe)								
Steel	**C**	**Mn**	**P**	**S**	**Si**	**Cr**	**Ni**	**Mo**	**N**
304	0.08 max	2.00	0.045	0.030	1.00 max	18.00–20.00	8.00–10.50	-	0.10
316L	0.03 max	2.00	0.045	0.030	0.75	16.00–18.00	10.00–14.00	2.00–3.00	0.10
2205	.030	2.00	0.030	0.020	1.00	22.00–23.00	4.5–6.5	3.00–3.50	0.14–0.20
3CR12	0.03 max	1.50 max	0.040 max	0.030 max	1.00 max	10.50–12.50	0.30–1.50	-	0.030

into metal particles and graphite, often called 'coke'. There are often carbonaceous filaments[17]. It usually occurs when hydrocarbons or a strong carburizing atmosphere, with a carbon activity much higher than unity activity, when the carbides are equilibrated with graphite. The iron carbides involved are metastable, e.g. Fe_3C[17] or Fe_5C_2[18].

Pitting has been associated with metal dusting when it occurs around 400–800°C and in an environment involving hydrocarbons or a strong carburizing atmosphere[15,16,17]. Variables that affect metal dusting include alloying elements, microstructures, as well as surface conditions[19,20,21]. Chromium, aluminium and silicon can increase the resistance to metal dusting, although the effect of carbide-formers, e.g. Ti and Nb is less substantiated[20,22,23].

For 316, the segregation of impurities such as K, S or Si at the grain boundaries also can cause sensitization, even without the segregation of Cr[24]. The presence of oxides and other corrosion products has been reported at high temperatures with water[25], and at the crack sides[26]. The corrosion products can accelerate the cracking because after forming, they can also act as crack initiation sites, enhancing crack propagation further[26]. Cookson *et al*.[27] showed that the intergranular cracking occurred by the mechanical failure of oxide particles, which created electrochemical crevices and stress concentrators, which both allow the intergranular cracks can initiate and propagate.

The Cr_3C_2, M_7C_3, M_6C, $M_{23}C_6$, R, chi, chromite, graphite and austenite phases were identified in metal dusted 316 using XRD and TEM[28]. Early in the exposure of the 316 wire to the high carbon activity atmosphere, the carbon diffused more readily along grain boundaries and dislocations. As the near surface region became saturated with carbon, segregation occurred, with the strong carbide formers such as chromium precipitating out mainly as M_6C or $M_{23}C_6$ carbides. This meant that the chromium depleted matrix had increased susceptibility to corrosion and could not heal the protective oxide film at the defects. Other phases such as R and chi also created chromium depletion in the matrix. With increased carbon content, more carbon-rich precipitates, such as M_7C_3 and Cr_3C_2, formed. The Cr_3C_2 phase had the highest occurrence in the smaller sized carbides formed later in metal dusting. No carbides had survived into the coke, although graphite coated chromite and austenite particles were found. Copper has also been reported to segregate between the oxide layer and the matrix in 316 steel[29].

Manganese and molybdenum can affect the pitting corrosion resistance of 304 and 316 stainless steels in chloride-containing media[30]. Molybdenum additions were beneficial because they became part of the passive film, protecting it from breakdown by aggressive Cl-ions, and the formation of Mo insoluble compounds in the aggressive pit environment facilitated the pit re-passivation. Conversely, manganese additions were deleterious, because MnS inclusions formed, and became pitting initiators.

Type 304 austenitic stainless steels are well known for being susceptible to intergranular corrosion, especially after exposure at 500–800°C, due to the precipitation of $Cr_{23}C_6$ which forms on the grain boundaries and depletes the surrounding matrix near those grain boundaries of the protecting Cr. The Cr depleted regions undergo preferential anodic dissolution and this is the reason for the accelerated intergranular attack. Jain *et al*.[31] found that the sensitization in 0.5M H_2SO_4 + 0.01M KSCN at 30°C increased rapidly up to 5 days before increasing more slowly.

Chang and Tsai[32] compared the different metal dusting behaviours between 304L and 347. Large pits formed on 304L and 347 stainless steels after exposure in 35% CO+ 60% H_2 +5% H_2O gas at 600°C for 500 h, and the 304L pits were deeper than in 347 SS. The particles left after metal dusting reaction were mostly Fe and Ni, with negligible Cr. At the bottom of the pits, were thick layers of coke, comprising carbon and disintegrated Fe/Ni particles, then a thin oxide, and a Cr-depleted precipitate-free zone with voids. Massive matrix carbide precipitation occurred below the Cr-depleted zone, and the carbide particle frequency decreased with increasing distance from the bottom of the pits. A continuous surface oxide film was apparently protective, because no carbides were observed beneath. In a study on 310 stainless steels, Yin[33] found that below 1 000°C, there was external carburization, oxidation, and internal carburization, and above 1 000°C, extensive external carburization occurred and internal Cr-carbides disappeared. Szakalos *et al*.[34] showed that the dusting was associated with discoloration around the shallow pits which looked like stains, and was very similar to the appearance of the 2205 coupon.

Oxidation and carburization behaviour of 304 stainless steel was studied during thermal cycling in CO/CO_2 at 700°C, and also in $CO/H_2/H_2O$ at 680°C by Zhang *et al*.[35]. They found that thermal cycling caused repeated scale separation, which accelerated the chromium depletion from the subsurface regions. The CO/CO_2 gas, with a carbon activity of 7 and pO_2 ¼ 10^{23} atm, caused internal precipitation of oxides and carbides, some surface damage, but no dusting. In contrast, the $CO/H_2/H_2O$ gas, with a C activity of 19 and pO_2 ¼ 5:4 10^{25} atm, caused rapid graphite deposition and metal dusting. This was accompanied by internal oxidation and carburization. The internal oxide was identified as spinel, which formed initially. Spinel formation badly affected the surfaces in both atmospheres, because it has a higher volume, and causes local expansion. In $CO/H_2/H_2O$, however, direct graphite deposition and metal disintegration into dust was the main reaction. Thermal cycling led in both cases to repeated scale spallation and, eventually, gas access to the underlying metal. The subsequent reactions between the substrate and carbon were very different in the two gases: entirely internal carbide precipitation in CO/CO_2, but principally graphite deposition in $CO/H_2/H_2O$.

The 3CR12 steel is classified as ferritic, because it has a higher proportion of ferrite, and the austenite precipitates within the ferrite, then transforms to martensite. It is often used because it is cost-effective in moderately corrosive environments. Type 3CR12 has excellent corrosion resistance at ambient temperatures, due to its 11–12%Cr. A depletion of Cr and enrichment of Ni and Mn in the martensite has been observed after exposure[36]. Also non-metallic inclusions and manganese sulphides can reduce the pitting potential and so allow micro-pits[37].

In general, 3CR12 has been recommended for moderately aggressive environments, with conditions as: pH 4–7; Cl- < 500 mg per litre; suspended solids < 200 mg per litre in flowing water[38] for ambient temperatures, although at elevated temperatures, these conditions are less likely to be sustained.

Perkins[39] found that failure in chloride containing environments was from corrosion pits, and a stress was necessary to initiate the pit. This might not be relevant in

this case, because it was shown that the stress had to be cyclic (i.e. corrosion fatigue), unless the stress could have risen from thermal cycling. Pitting corrosion resistance in de-aerated 3.5% NaCl solution was improved for both hot-rolled and annealed 3CR12 steel using a laser surface melting (LSM) technique[40].

Duplex stainless steels, such as 2205, are increasingly being used as structural materials where high mechanical strength is required in highly corrosive environments e.g. like chemical plants, offshore platforms, oil and gas production and process systems[41–43]. The good properties arise from the two phases, austenite and ferrite, and the required balance is achieved by a heat treatment in the two-phase region. Any subsequent heat treatment may lead to a marked change in the proportions of the phases, and degrade the beneficial properties. Since the new generation duplex stainless steels contain very low carbon, intergranular corrosion due to the carbide precipitation in these steels, and the ensuring grain boundary sensitization and cracking, should not be a serious problem. However, there can be precipitation of sigma and other intermetallic compounds at the grain boundaries, which can encourage intergranular cracking (IGC)[41,44,45]. This occurs because sigma is richer in chromium and molybdenum than either the austenite or ferrite of the solution treated alloy, and so depletes those elements in the surrounding matrix.

In a study of the effect of cooling rates on welded SAF 2205 alloys[46], found many small pits, 10–20 microns in the heat-affected zone (HAZ) of both sets of samples. Austenite grains were reported as being more resistant to a chloride environment than the ferritic matrix[47], and the initiation sites for the pits were identified as being at the ferrite-austenite grain boundaries, from whence the pits grew rapidly initially to the adjacent ferrite, and then into austenite. The cooling rates were found to affect the corrosion resistance by the alteration of the microstructure. Fast cooling promotes a near continuous network of intergranular allotriomorphic austenite, which engulfed the ferrite grains, and this network was discerned to be more corrosion resistant[46]. It was concluded that welding did not significantly alter the intergranular corrosion behavior of the SAF 2205 steel, but reduced pitting corrosion resistance. Young *et al.*[48] investigated the effect of hydrogen embrittlement on notched tensile strength (NTS) and fracture characteristics of 2205 duplex stainless steel welds. All the specimens were susceptible to gaseous hydrogen embrittlement, but the susceptibility decreased with increasing austenite content in the weld metal.

Sozańska and Kłyk-Spyra[49] studied the effect of isothermal treatment (at 675°C, 750°C and 900°C) on hydrogen induced cracking (HIC) in sour environments containing hydrogen sulphide of a 2205 duplex stainless They found that 2205 containing nearly 12 vol.% of σ phase in dispersed conditions was resistant to step cracking in wet environments containing hydrogen sulphide. It was highly possible that a crack would propagate faster along the embrittled σ phase, although very small cracks were found at austenite-ferrite boundaries where σ phase particles were present.

Now that stainless steels containing high manganese and nitrogen contents are manufactured, new formulae incorporating their effects in pitting resistance equations (PRE) have been developed, but although Mn is taken as deleterious, no one formula is generally accepted, so it is not included below. When both Mo and N are present, they contribute synergistically to improving pitting corrosion and crevice corrosion resistance[50–52]. The decreasing solubility of N at high contents must be considered. Thus, Jargelius-Petersson[50] proposed a new PRE formula:

$$PRE = \%Cr + 3.3\%Mo + 51\%N + 6\%Mo\%N - (1.6\%N)^2$$

This gave PRE values (rounded up) as: 14 or 3CR12; 35 for 316L; 25 for 304; and 49 for 2205, which are slightly different from derived before, but still giving the same rankings. However, the calculation does not always give meaningful results for stainless steels with more than one constituent phase, e.g. duplex stainless steels. Perren *et al.*[53] demonstrated that the pitting resistance of duplex stainless steels should be quantified by using the PRE of the weaker phase, which can either be ferrite or austenite[53,54]. It has long been known[55] that silicon slows the rate of carburization, even under gas conditions where no silicon-rich oxide can form.

Overall, the conditions were very harsh, and at much higher temperatures than for which these steels are usually recommended. Apart from the carbon steel, which disappeared totally, the stainless steels all had similar metallographic features, albeit in differing amounts. All had intergranular corrosion and carbide precipitation. Similarly, all the stainless steels show some carbide precipitation, and this was often ahead of the cracking, which is associated (indeed, the principal cause) with sensitization. Both the 3CR12 and 2205 coupons had less penetrating intergranular corrosion, and had more general attack, with a scale on the surface.

There are many similarities with the metal dusting phenomenon, which is also related to direct reduction of iron (DRI). In this degradation type, as well as the carbide precipitation along the grain boundaries and the intergranular corrosion, there were also layers formed externally (albeit for different thicknesses). Dusting typically starts under these layers, as it did for 316L and 304. Type 316L had graphite nodules (easily identified in the unetched microstructure), and some fairly large pits (~200 μm deep), which did not have the classic large pit under a small surface hole, that is normally associated with chlorine ion attack. There was also spalling of a layer in 316L, which is also associated with metal dusting. The high flow rates would have removed much of the corrosion product, for example, loose spalling, the 'dust' comprising the carbide, graphite and metal particles, as well as any filaments. Metal dusting is a runaway mechanism once it reaches a critical threshold, and then there is very little that can arrest it. It is likely that the mechanism was mainly metal dusting, although there is grain boundary carbide precipitation and subsequent intergranular corrosion (i.e. classic sensitization, with the possibility of stress corrosion cracking), and that the corrosion was in the fairly early stages, before 'runaway'. This agrees with the thin external layers observed. The environment is suitable for metal dusting (reported for atmospheres comprising CO_2, CO, H_2 and H_2O mixtures[56]), although the spigot was exposed to N_2 as well, and there were only small amounts of O_2 and H_2O), although the operation temperatures is much higher that reported.

In the spigot, the best alloys were 316L and 2205 which lasted well during the second campaign of ~10 months. However, 316L was reported to have severe coarse pitting during the first campaign which lasted 6 months. The difference in environments between the two campaigns is that the spigot was expected to have reached higher

temperatures in the second campaign since the water-cooling had been blocked. Thus, counter intuitively, it appeared that the higher temperatures were actually more protective.

More work is needed to find an optimum alloy, and possibilities include 2205 with cathodic modifying additions[57], or more specialized alloys developed for higher temperature applications. Although a refractory lining would remove the corrosion problems, it would necessitate the need for lancing which increases operation time, as well as increasing the thermal stress on the alloy.

Conclusions

The spigot had obviously reached higher temperatures than its designed conditions. This had occurred because the cooling system had been plugged. Also the inside had been refractory lined which allowed more insulation, but resulted in more regular mechanical cleaning, which the original design was avoiding. All the alloys were being used at much higher temperatures than is usual.

Coarse pitting had been experienced on the original 316L stainless steel, and a repair at Mintek involved refractory casting, and a lower region of plates of 316L. Simultaneously, the opportunity was taken to fit eight experimental coupons inside the spigot in two different locations for the comparison of four different steels.

Nearest the arc, but in a more sheltered location where thermal cycling is more likely, none of the coupons had survived. Unfortunately, it could not be discerned whether this was due to weld failure, or the coupon failure. On the side away from the arc, the 2205 stainless steel had survived and two others were found as stumps. The plain carbon steel, was missing completely. The 316L repair plates had also survived well, even though it had been severely pitted in the earlier campaign.

Microstructural examination of the 316L repair plates and the remaining coupons showed that the alloys had carbide precipitation, with highest incidence on 316L and 304. This is classic sensitization, and is also associated with stress corrosion cracking. The spigot could have been stressed because of the thermal cycling which would have occurred when the plant was shut down for maintenance, although the high temperatures might have allowed some stresses to be annealed out.

All alloys showed layers at the surface, and 316 also had graphite nodules and spalling of metal layers. Together with the grain boundary attack, this is also symptomatic of the first stages of metal dusting, before the reaction becomes ‘runaway’. The conditions were suitable for metal dusting, although the exact temperatures too which the inside of the spigot was subjected is unknown.

To avoid the use of a refractory material, it is likely that another specifically designed high temperature alloy would be used.

References

1. Denton, G.M. Private communication.
2. Visual Inspection of Water Cooled Duct Sections, 3 April 2009, ENVIROPLUS DESIGN.
3. NDE Catalogue for the Chemical, Petrochemical and Manufacturing Industry.
4. Technical Data for CS2205, Columbus Steels, www.columbusstainless.co.za
5. ABOU-ELAZM, A., ABDEL-KARIM, R., ELMAHALLAWI, I. and RASHAD, R., Correlation between the degree of sensitization and stress corrosion cracking susceptibility of type 304H stainless steel, *Corrosion Science* 2009, vol. 51, pp. 203–208 .
6. ABOU-ELAZM, A., ABDEL-KARIM, R., ELMAHALLAWI, I. and RASHAD, R., *Engineering Failure Analysis*, 2009, vol. 16, p. 433.
7. BAIN, E.C., ABORN, R.H. and RUTHERFORD, J.J.B., The nature and prevention of intergranular corrosion in austentic stainless steels, *Transactions of the American Society for Steel Treating*, 1933, vol. 21, pp. 481–509.
8. ZAHUMENSKY, P., TULEJA, S., ORSZAGOVA, J., JANOVEC, J. and SILADIOVA, V., *Corrosion Science*, 1999, vol. 41, p. 1305.
9. PADILHA, A.F., ESCRIBA, D.M., MATERNA-MORRIS, E., RIETH, M. and KLIMENKOV, M., *Journal of Nuclear Materials*, 2007, vol. 362, p. 132.
10. TERADA, M., ESCRIBA, D.M., COSTA, I., MATERNA-MORRIS, E. and PADILHA, A.F., *Materials Characterization*, 2008, vol. 59, p. 663.
11. NAGAE, Y. *Materials Science and Engineering* A, 2004, vols. A387–389, p. 665.
12. ARIOKA, K., YAMADA, T., TERACHI, T. and STAEHLE, R.W., *Corrosion*, 2006, vol. 62, p. 74.
13. BELTRAN, R., MALDONADA, J.G., MURR, L.E. and FISHER, W.W., *Acta Materialia*, 1997, vol. 45, p. 4351.
14. ALMANZA, E. and MURR, L.E., *Journal of Materials Science*, 2000, vol. 35, p. 3181.
15. HOYT, W.B. and CAUGHEY, R.H. High temperature metal deterioration in atmospheres containing carbon-monoxide and hydrogen, *Corrosion*, 1959, vol. 15, pp. 627t–630t.
16. LEFRANCOIS, P.A. and HOYT, W.B., *Corrosion*, 1963, vol. 19, p. 360t.
17. GRABKE, H.J., KRAJAK, R. and NAVA PAZ, J.C. On the mechanism of catastrophic carburization: 'metal dusting', *Corrosion Science*, 1993, vol. 35, pp. 1141–1150.
18. WEI, Q., PIPPEL, E., WOLTERSDORF, J. and GRABKE, H.J. Materials and Corrosion, 1999, vol. 50, pp. 628–633.
19. GRABKE, H.J. and MULLER-LORENZ, E.M. *Materials Corrosion*, 1998, vol. 49, pp. 317–320.
20. MULLER-LORENZ, E.M., STRAUSS, S., and GRABKE, H.J. Effects of surface state, microstructure and alloying additions on the metal dusting resistance of high alloy steels, *Eurrocorr 98, The European Corrosion Congress,* Sept. 28–Oct. 1, 1998, Utrecht, Netherlands, 1998, no. 24.
21. GRABKE, H.J. *Material Science Forum*, 2001, vols. 369–372, p. 101.
22. STRAUSS, S., and GRABKE, H.J., Role of alloying elements in steels on metal dusting, *Materials Corrosion*, 1998, vol. 49, pp. 321–327.
23. SCHNEIDER, A., and ZHANG, J., *Materials Corrosion*, 2003, vol. 54, p. 778.
24. ARMIJO, J.S. *Corrosion*, 1968, vol. 8, p. 24.

25. ANDERSON, P.L. *Corrosion Science*, 1993, vol. 49, p. 14.

26. STROOSNIJDER, M.F., GUTTMANN, V., and DE WIT, J.H.W. *Metall. Mater. Trans. A*, 1995, vol. 26A, p. 2103.

27. COOKSON, M., WAS, G.S., and ANDERSON, P.L. *Corrosion Science*, 1998, vol. 54, p. 4.

28. STEVENS, K.J., LEVI, T., MINCHINGTON, I., BRIGGS, M., KEAST, V. and BULCOCK, S. Transmission electron microscopy of high pressure metal dusted 316 stainless steel, *Materials Science and Engineering A*, 2004, vol. 385A, pp. 292–299.

29. HUANG, Y.Z. and TITMARSH, J.M. *Acta Materiala*, 2006, vol. 54, pp. 635– 642.

30. PARDO, A., MERINO, M.C., COY, A.E., VIEJO, F., ARRABAL R. and MATYKINA, E. Pitting corrosion behaviour of austenitic stainless steels—combining effects of Mn and Mo additions, *Corrosion Science*, 2008, vol. 50, pp. 1796–1806.

31. JAIN, S., BUDIANSKY, N.D., HUDSON, J.L., and SCULLY, J.R. Surface spreading of intergranular corrosion on stainless steels, *Corrosion Science*, 2010, vol. 52, pp. 873–885.

32. CHANG, C.-H and TSAI, W-T. Carburization behavior under the pits induced by metal dusting in 304L and 347 stainless steels, *Materials Chemistry and Physics*, 2009, vol. 116, pp. 426–432.

33. YIN, R. Carburization of 310 stainless steel exposed at 800–1 100°C in 2%CH_4/H_2 gas mixture, *Corrosion Science,* 2005, vol. 47, pp. 1896–1910.

34. SZAKALOS, P., PETTERSSON, R., and HERTZMAN, S. An active corrosion mechanism for metal dusting on 304L stainless steel, *Corrosion Science*, 2002, vol. 44, pp. 2253–2270.

35. ZHANG, J., BODDINGTON, K., and YOUNG, D.J. Oxidation, carburisation and metal dusting of 304 stainless steel in CO/CO_2 and $CO/H_2/H_2O$ gas mixtures, *Corrosion Science*, 2008, vol. 50, pp. 3107–3115.

36. KNUTSEN, R.D. *Materials Science and Technology*, 1992, vol. 8, p. 621.

37. KNUTSEN, R.D., and HUTCHINGS, R. *Materials Science and Technology*, 1988, vol. 4, p. 127.

38. McEWAN, J.J., KINCER, M.U., SCHEERS, P.V.T, and WHITE, R.T. Intuition, case work and testing: a holistic approach to the corrosion of a 12% chromium steel in aqueous environments, *Corrosion Science*, 1993, vol. 35, pp. 303–315.

39. PERKINS, K.M., and BACHE, M.R. Corrosion fatigue of a 12%Cr low pressure turbine blade steel in simulated service environments, *International Journal of Fatigue*, 2005, vol. 27, pp. 1499–1508.

40. CHONG, P.H., LIU, Z., SKELDON, P., and CROUSE, P. Characterisation and corrosion performance of laser-melted 3CR12 steel, *Applied Surface Science*, 2005, vol. 247, pp. 362–368.

41. HERBSLEB, G., and SCHWAAB, P. *Duplex Stainless Steels*, R.A. Lula (ed.), p. 15. ASM, Ohio 1983.

42. STREICHER, M.A. *Metal Progress*, 1985, vol. 128, p. 29.

43. SRIDHAR, N., KOLTS, J., and FLASHE, L.H. *Metals*, 1985, vol. 37, p. 31.

44. DEBOLD, T.A. *Journal of Metals*, 1989, vol. 41, p. 12.

45. RAVINDRANATH, K., and MALHOTRA, S.N., The influence of aging on the intergranular corrosion of 22 chromium-5 nickel duplex stainless steel, *Corrosion Science*, 1995, vol. 37, pp. 121–132.

46. KORDATOS, J.D., FOURLARIS, G., and PAPADIMITRIOU, G., The effect of cooling rate on the mechanical and corrosion properties of SAF 2205 (UNS 31803) duplex stainless steel welds, *Scripta Materiala*, 2001, vol. 44, pp. 401–408.

47. SRIRAM, S., and TROMANS, D. *Corrosion*, 1999, vol. 45, p. 804.

48. YOUNG, M.C., CHAN, S.L.I., TSAY, L.W., and SHIN, C.-S. Hydrogen-enhanced cracking of 2205 duplex stainless steel welds, *Materials Chemistry and Physics*, 2005, vol. 91, pp. 21–27.

49. SOZAŃSKA, M., and KŁYK-SPYRA, K. Investigation of hydrogen induced cracking in 2205 duplex stainless steel in wet H_2S environments after isothermal treatment at 675, 750 and 900°C, *Materials Characterization*, 2006, vol. 56, pp. 399–404.

50. JARGELIUS-PETTERSSON, R.F.A. *Corrosion*, 1998, vol. 54, p.162.

51. OLSSON, C.-O.A. Corrosion Science, 1995, vol. 37, p. 467.

52. OLEFJORD, I., and WEGRELIUS, L. *Corrosion Science*, 1996, vol. 38, p. 1203.

53. PERREN, R.A., SUTER, T.A., UGGOWITZER, P.J., WEBER, L., MAGDOWSKI, R., BOHNI, H., and SPEIDEL, M.O. Corrosion resistance of super duplex stainless steels in chloride ion containing environments: investigations by means of a new microelectrochemical method: I, *Corrosion Science*, 2001, vol. 43, p.707.

54. PERREN, R.A. SUTER, T.A., SOLENTHALER, C., GULLO, G., UGGOWITZER, P.J., BOHNI, H., and SPEIDEL, M.O. Corrosion resistance of super duplex stainless steels in chloride ion containing environments: investigations by means of a new microelectrochemical method: II. Influence of precipitates, *Corrosion Science*, 2001, vol. 43, pp. 727–745.

55. KANE, R.H. *Corrosion*, 1981, vol. 37, p.187.

56. GRABKE, H.J., KRAJAK, R., and NAVA PAZ, J.C. *Corrosion Science*, 1993, vol. 35, p. 1141.

57. POTGIETER, J.H., SKINNER, W., and HEYNS, A.M. The nature of the passive film on cathodically modified stainless steels, *Journal of Applied Electrochemistry*, 1993, vol. 23, pp. 11–18.

Prof. Lesley Alison Cornish

Professor, Director: DST/NRF Centre of Excellence in Strong Materials, University of the Witwatersrand, DST/NRF Centre of Excellence in Strong Materials

Lesley Cornish has been deriving phase diagrams and undertaking alloy development work for over 25 years, starting with her PhD. Apart from four years at the United Kingdom Atomic Energy Authority and six years at Mintek, most of her working life was at the University of the Witwatersrand. She has lectured all undergraduate years and post graduate students on Physical Metallurgy, and supervised over 32 students, of whom 24 have graduated, many of whom went to work in research. She has worked with platinum group metals, steels, WC-VC-Co hardmetals and aluminium alloys. She has written over 70 papers in journals, over 120 conference proceedings, about 60 research reports and one provisional patent. She has been working with Materials Science International for 10 years, contributed to 7 books on phase diagrams, and co-wrote a chapter in the ASM Handbook on Metallography for 2004. She is the Director of the DST/NRF Centre of Excellence in Strong Materials (CoE-SM), and was instrumental in the establishment of the African Materials Science and Engineering Network (AMSEN) in 2008. Both the CoE-SM and AMSEN encourage her passions: research and developing people. She is also Assistant Dean - Research in the Faculty of Engineering and the Built Environment at Wits. She won the Vice-Chancellors Teaching Award (Wits) in 1998 and has won the Best Published Electron Microscopy Paper Prize from the Microscopy Society of Southern Africa five times. She also enjoys wildlife and travelling to places without cell. phone reception!